Commun. Comput. Chem. Vol.**2**, No.**3**, pp.117-130
doi: 10.4208/cicc.2014.v2.n3.3 Oct 2014

REGULAR ARTICLE

A New Excited-State Intramolecular Proton Transfer Mechanism for C2 Symmetry of 10-hydroxybenzoquinoline

Jinfeng Zhao, Peng Song*, Fengcai Ma*

Department of Physics and Chemistry, Liaoning University, Shenyang 110036, P. R. China
Received 15 Sep 2014; Accepted (in revised version) 8 Oct 2014

Abstract: The excited state intramolecular proton transfer (ESIPT) mechanisms of bis-phenol possessing C_2 symmetry of 10-hydroxybenzoquinoline (2HBQ-a) have been investigated based on the time-dependent density functional theory (TDDFT). A new ESIPT mechanism of concomitant single and double ESIPT process has been proposed, which is different from the one proposed previously (Piechowska *et al*. *J. Phys. Chem. A*. 2014, **118**, 144). The phenomenon of hydrogen bond strengthening was verified based on primary bond lengths, angles and the IR vibrational spectra. The calculated vertical excitation energies based on the TDDFT method reproduced the experimental absorbance and fluorescence emission spectra well. Three stable structures of 2HBQ-a tautomerization have been founded in the S_1 state. Intramolecular charge transfer based on the frontier molecular orbitals demonstrated the indication of the ESIPT reaction. The constructed PESs of S_0 and S_1 states based on keeping the O-H distance fixed at a serious of values have been used to illustrate the ESIPT process. The values of potential barriers among these stable points in the S_1 state are less than 10 kcal/mol, which infer a concomitant single and double proton transfer mechanism. Based on the new ESIPT mechanism, we further explained the phenomenon of fluorescence quenching reasonably.

AMS subject classifications: 74E40, 78M50
Keywords: Excited-State Intramolecular Proton Transfer; Electronic Spectra; Frontier Molecular Orbitals; Potential Energy Surface;

* Corresponding author. *Email address*: songpeng@lnu.edu.cn (P. Song)
fcma@lnu.edu.cn (F. –C. Ma)

1. Introduction

Excited-state intramolecular proton transfer (ESIPT), as one of the most important elementary reactions in chemistry and biology [1-7], is the pioneering work of Weller *et al.* [8, 9]. A new kind of investigation, the unique observation of methyl salicylate in the field of photochemistry, was envisaged in the middle of the last century [8, 9]. Since then, extensive studies on proton transfer (PT) reactions were performed both experimentally and theoretically [10-16]. PT occurs in molecules containing both acidic and basic groups that may rearrange in the electronic excited state via transferring a proton or hydrogen atom. The strong and fast reorganization of the charge distribution derived from tautomerization makes these molecules very attractive towards the design and use of fluorescence sensors [17–22], laser dyes and LEDs [23, 24], UV filters [25–27], and molecular switches [28, 29]. In effect, the excited state intra- or inter- molecular proton transfer is one of the simplest examples of a hydrogen bond reaction that occurs in electronically excited state. Recently, the hydrogen bonds between donor and acceptor in excited state upon photo-excitation have been researched based on the time-dependent density functional theory (TDDFT) by Han and co-workers theoretically [30-35]. That is to say, to further study the PT mechanism, DFT and TDDFT methods have been the primary tool to clarify fundamental aspects concerning the different electronic states and structures.

10-Hydroxybenzo[*h*]quinoline (HBQ), as an important reagent in the preparation of optical filter agents, has been payed attention to for a long time [36, 37]. The excited-state intramolecular proton transfer (ESIPT) of HBQ is a prototypical reaction in solution [38-45]. The enol form of HBQ is stable in the S_0 state, which converts from the enol to the keto form rapidly following photoexcitation. Takeuchi *et al*. reported the rate of ESIPT and the decay times of subsequent coherent vibrational motions in cyclohexane based on the pump-probe transient absorption spectroscopy firstly [38]. The ESIPT rate was about 25 fs and the decay time of a vibrational mode was at about 250 cm^{-1}, which was faster than the decay times of higher-frequency modes [38]. Subsequently, Takeuchi *et al*. proposed that the mode at 250 cm^{-1} was correlated with the ESIPT reaction. Similar experimental results were also reported by Schriever *et al*. [39]. Chou *et al*. reported the dynamics of excited-state intramolecular enol-keto proton-transfer HBQ based on steady-state absorption and fluorescence spectroscopy, femtosecond fluorescence up-conversion combining with pump-probe transient absorption experiments in detail [40]. Various PH dependent ESIPT dynamics of HBQ have been investigated in aqueous solution [41], which demonstrated the charge transfer between hydroxyl oxygen and benzoquinolinic nitrogen acting as a driving force for the proton transfer reaction. Robert *et al.* reported the influence of organized media of HBQ

based on the fluorescence probe technology in aqueous solution [42]. Higashi *et al.* investigated the ultrafast ESIPT reaction of HBQ based on the electronically embedded multi-configuration shepard interpolation method [43]. Subsequently, Lee *et al.* reported an active role of HBQ manifesting no isotope dependence implying complete passive role of the proton [44]. In brief, the study about ESIPT reaction of HBQ has been adept currently. Recently, an owning bis-phenol C_2 symmetry of 10-hydroxybenzoquinoline (2HBQ-a shown in Figure 1), a new synthetic molecule, has been used to investigate the ESIPT process in toluene solvent reported by Piechowska *et al*. [45]. Steady-state and time resolved fluorescence measurements were adopted demonstrating a single proton transfer process in S_1 state [45]. However, spectroscopic techniques, such as steady-state absorption spectroscopy, fluorescence spectroscopy and the time resolved fluorescence spectroscopy, provide only indirect information about photophysical proterties. In fact, there are some questionable points worth investigating deeply. For this kind of C_2 symmetry structures, whether the double proton transfer was more likely to happen rather than the single proton transfer. In addition, the Fluorolog 3 fluorometer (SPEX Inc.) has a restriction that the emission detection range is only 450-840 nm [45]. Therefore, in order to get a clear and detailed picture of ESIPT mechanism, in the present work, a theoretical investigation has been adopted to study both the S_0 and the S_1 state of molecular relevant to the transfer mechanism based on the DFT and the TDDFT method, respectively. The configurations of S_0 state and S_1 state were optimized, and further vertical excitation energies, IR vibration spectra, the frontier molecular orbitals and homologous S_0 and S_1 states potential energy surfaces (PESs) were calculated and analyzed to provide the direct information of the ESIPT process.

2. Computational Details

In the present work, all the theoretical calculations presented here were accomplished based on the DFT and TDDFT methods with Becke's three-parameter hybrid exchange function with the Lee–Yang–Parr gradient-corrected correlation functional (B3LYP) [46-52] as well as 6-31+G (d) basis set by Gaussian 09 programs [53]. The TD-DFT method has become a very useful tool to research the hydrogen bonding in the excited states of the hydrogen-bond system theoretically [30-35, 54-59]. Because the experiments were conducted in a solvent, in all calculations the solvent effect (toluene) were based on the Polarizable Continuum Model (PCM) using the integral equation formalism variant (IEF-PCM) [60-63]. The geometries of S_0 and S_1 states for the 2HBQ-a, 2HBQ-b and 2HBQ-c were optimized without constrain of bonds, angles and dihedral angles. Vibrational frequency calculations have been used to analyze the optimized structures to confirm that these structures corresponded to the local

minima on the S_0 and S_1 PESs (no imaginary frequency).The calculations of vertical excitation energies were also performed from the ground-optimized structures based on TDDFT methodology with IEF-PCM, and our theoretical calculations predicted the six low-lying absorbing transitions. The S_0 and S_1 PESs of the 2HBQ-a have been scanned by constrained optimizations and frequency analyses to obtain the thermodynamic corrections in the corresponding electronic state, and keeping the O_1-H_2 and O_4-H_5 lengths fixed from 0.69 to 1.99 Å.

Fine quadrature grids of size 4 were employed. The self-consistent field (SCF) convergence thresholds of the energy for both the ground state and excited state optimization were set at 10^{-8} (default settings are 10^{-6}). Harmonic vibrational frequencies in the ground and excited state were determined by diagonalization of the Hessian. The excited-state Hessian was obtained by numerical differentiation of the analytical gradients using central differences and default displacements of 0.02 Bohr. The infrared intensities were determined from the gradients of the dipole moment [52].

3. Results and discussion

3.1 Optimized Structures

In order to consider all possible structures involved in the proton transfer process, we optimized out three stable structures. Both the S_0 state and the S_1 state structures of the 2HBQ-a, 2HBQ-b and 2HBQ-c were obtained at the B3LYP function with 6-31+G (d) basis set level of theory (seen in **Figure1**), with a subsequent vibrational frequency analysis to ensure

Table 1: The calculated primary bond lengths (Å) and angles (º) of 2HBQ-a, 2HBQ-b and2HBQ-c in the S_0 state and S_1 state based on the DFT and TD-DFT methods, respectively.

	2HBQ-a		2HBQ-b		2HBQ-c	
Electronic state	S_0	S_1	S_0	S_1	S_0	S_1
O1-H2	0.999	1.035	1.595	1.708	1.622	1.708
H2-N3	1.695	1.585	1.059	1.044	1.054	1.041
O4-H5	0.999	1.035	0.997	1.008	1.622	1.708
H5-N6	1.695	1.585	1.707	1.667	1.054	1.041
δ(O1-H2-N3)	147.1º	150.3º	142.7º	140.4º	141.6º	142.7º
δ(O4-H5-N6)	147.1º	150.3º	146.8º	140.4º	141.6º	142.7º

the validity of the stationary points. The toluene solvent was selected in the IEFPCM model insuring consistency with the experiment [45]. In addition, some fundamental structure parameters (primary bond lengths (Å) and angles) of these three stable structures have been shown in **Table 1**. To describe more clearly below, We labeled a serial numbers from 1 to 6 on the atoms connected to the hydrogen bonds. It is worth noting that the calculated lengths of O_1-H_2, H_2-N_3 (H_2···N_3), O_4-H_5 and H_5-N_6 (H_5···N_6) of 2HBQ-a structure are 0.999, 1.695, 0.999 and 1.695 Å in the S_0 state, respectively. However, in the S_1 state, these bond lengths are changed to be 1.035, 1.585, 1.035 and 1.585 Å. The variable-length O_1-H_2 and O_4-H_5 bands as well as variable-short H_2···N_3 and H_5···N_6 indicate that the two intramolecular hydrogen bonds are strengthened in S_1 state. Moreover, the bond angle δ (O-H-N) changes from 147.1º in the S_0 state to 150.3º in the S_1 state, which also can be used as one of the indications of hydrogen bond strengthening. In effect, the hydrogen bond strengthening or weakening can also be revealed based on monitoring the spectral shifts of some characteristic vibrational modes involved in the formation of hydrogen bonds [30-35, 54-59]. **Figure 2** revealed the vibrational spectra of 2HBQ-a in the conjunct vibrational regions of the O–H stretching modes, which demonstrates that the intramolecular hydrogen bonds O_1-H_2···N_3 and O_4-H_5···N_6 induces a large red-shift of O-H stretching frequency in the S_1 state. In the S_0 state, the calculated O-H stretching vibrational frequency is located at 3162 cm^{-1}, whereas it is located at 2535 cm^{-1} in the S_1 state. The large red-shift of 627 cm^{-1} could be concluded due to the effect of the excited-state intramolecular hydrogen bonds O_1-H_2···N_3 and O_4-H_5···N_6. It further indicates the two intramolecular hydrogen bonds are strengthened.

3.2 Electronic spectra and Frontier Molecular Orbitals (MOs)

The calculated electronic spectra (absorption and emission spectra) of these three stable

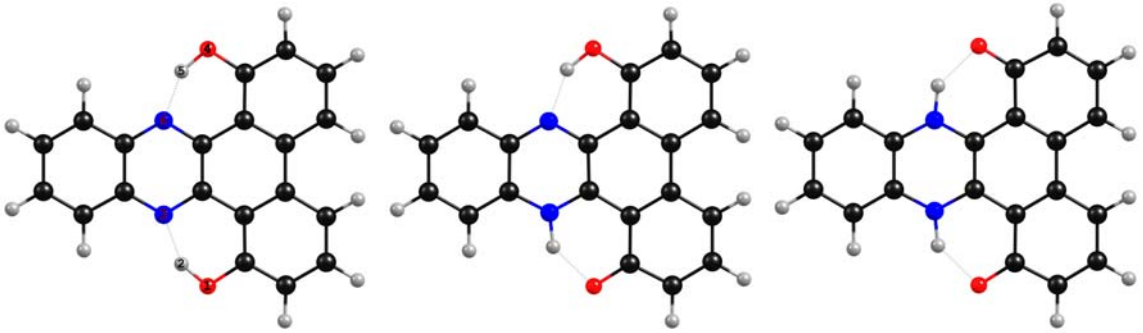

2HBQ-a 2HBQ-b 2HBQ-c

Figure 1: The optimized structures of the ground state for 2HBQ-a, 2HBQ-b and 2HBQ-c at TDDFT/B3LYP/6-31+G (d) level. Red: O; Gray: H; Blue: N; Aqua: C.

structures were displayed in **Figure 3** based on the TDDFT/B3LYP/6-31+G (d) level. It should be noted that the absorption hump of 2HBQ-a is located at 434 nm, which agrees well with 429 nm based on the experiment [45]. The emission hump was calculated at 482 nm. The bathochromic-shift of 48 nm corresponding to absorption peak can be ascribed to the Stokes shift. Moreover, due to another emission hump of 722nm reported based on the experiment [45] and they assigned it to the fluorescence peak of 2HBQ-b. In order to verify the theoretical calculations adopted is reasonable and effective, we found the emission hump of 2HBQ-b was located at 720 nm that is in good agreement with the experimental result [45]. On the contrast, a fluorescence peak of 869 nm was founded based on the stable structure 2HBQ-c, which was not reported by experiment. It should be attributed to the restriction of the Fluorolog 3 fluorometer (SPEX Inc.), which just has an emission detection rang of 450-840 nm [45]. On account of the accurate theoretical calculations, the emission peak of 869 nm really exists; the single proton transfer in S_1 should be questionable [45]. Therefore, it is necessary to restudy the ESIPT mechanism of 2HBQ-a chromophore in detail. In fact, the ESIPT process of this chromophore may be two pathways: One is the single ESIPT process, the other is the double ESIPT process. If the potential barrier between 2HBQ-a and 2HBQ-c is too high to cross, the single ESIPT occurs. If the potential barrier between them is lower enough to cross, the double ESIPT may occur.

Figure 4 displays the calculated frontier molecular orbitals (MOs) of the 2HBQ-a in toluene solvent to depict the nature of the electronically excited state. Only the highest occupied molecular oribital (HOMO) and the lowest unoccupied molecular oribital (LUMO) were shown here, since just these two orbitals are referred to in the S_1 state with the large oscillator strength of 0.3873. The π character for the HOMO as well as the π^* character for LUMO could be seen from **Figure 4** clearly. That is to say, a dominant $\pi\pi^*$-type transition could be assigned with the 97.6% composition from HOMO to LUMO. In addition, the

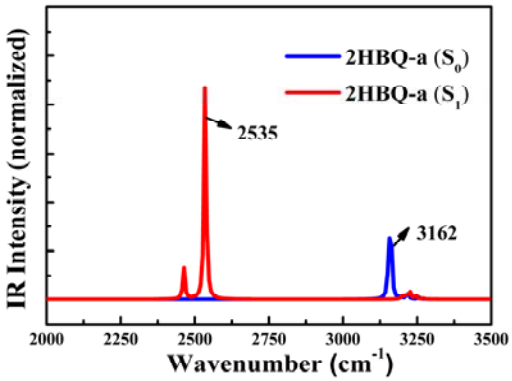

Figure 2: The calculated IR spectra of 2HBQ-a at the spectral region of both O-H stretching bands in S_0 and S_1 states at TDDFT/B3LYP/6-31+G (d) level.

electron density of the hydroxyl moiety decreases and the N atom increases after transition from the HOMO to LUMO. That is to say, the intramolecular charge transfer is involved in the S_1 state and the intramolecular hydrogen bonding (O_1-H_2···N_3 and O_4-H_5···N_6) can be influenced based on the change of electron density in the hydroxyl moiety directly. Therefore, the S_1 state ESIPT process could occur due to intramolecular charge transfer.

3.3 Potential energy surfaces

In order to reveal the detailed mechanism of the ESIPT process in the 2HBQ-a chromophore, all the S_0 state and S_1 state geometrical structures with fixed O_1–H_2 and O_4–H_5 bond lengths have been optimized at the DFT/B3LYP/TZVP level with the IEF-PEM solvation model of toluene. The constructed PESs in the S_0 and S_1 states as functions of the O_1–H_2 and O_4–H_5 bond lengths ranging from 0.69 to 1.99 Å among the 2HBQ-a structure are shown in **Figure 5**, respectively. Even though the correct ordering of the closely spaced excited state can not expected to be sufficiently accurate to yield based on the TDDFT method, previous calculations have demonstrated that the method could be reliable to provide qualitative energetic pathways for the proton transfer process [64-66]. The symmetrical PES of the S_0 state is shown in **Figure 5**(**b**) with four minimum points. The coordinates of these points are A (0.99 Å, 0.99 Å), B (0.99 Å, 1.69 Å) and C (1.69 Å, 1.69 Å), respectively. In fact, the A point is the most stable and the C point is least stable among these minimum points, which demonstrates that A point is favored in S_0 state. After excitation, the 2HBQ-a chromophore is excited to the S_1 state. In effect, it should be noted that the PES is also symmetrical (seen in **Figure 5**(**a**)) and four minimum points in the S_1 PES were found. In fact, due to the symmetry of S_1 PES, we only show three minimum points in this figure (A, B and C). The coordinates of these points are A (0.99 Å, 0.99 Å), B (0.99 Å, 1.69 Å) and C (1.69 Å, 1.69 Å),

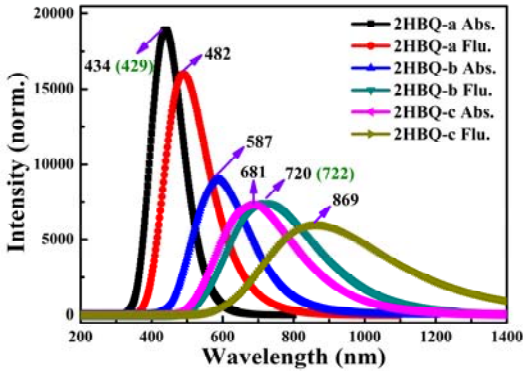

Figure 3: The calculated electronic spectra of 2HBQ-a, 2HBQ-b and 2HBQ-c in toluene solvent at TDDFT/B3LYP/6-31+G (d) level. The corresponding experimental values are given in the parentheses.

respectively. The calculated results demonstrated that the sizes of these potential energy relationship are: Ec (the potential energy of the C point) < E_B < E_A. In other words, the 2HBQ-c structure is the most stable and 2HBQ-a is the most volatile among these minimum points in S_1 state. That is to say, the ESIPT process is willing to happen in the S_1 state. To verify whether the single ESIPT process or the double ESIPT process would happen, we compare the potential barriers among these minimum points. The calculated results manifest that it is an almost no barrier process from A point to B point. And from A point to C point, it needs to cross the1.61 kcal/mol potential barrier. From B point to C point, it needs to cross the 3.42 kcal/mol potential barrier. Even though from A point to B point is a no barrier process, these calculated values of the potential barriers are not too large. Therefore, both the single ESIPT and double ESIPT processes could occur in the S_1 state. In addition, in order to consider more comprehensive, the reverse proton transfer potential barriers among these minimum points were also calculated in the S_1 state. From B point to A point, it needs to cross about 7.05 kcal/mol. And from C point to A point, it needs to cross the 7.6 kcal/mol. From C point to B point, it needs to cross the 0.55 kcal/mol. That is to say, the reverse proton transfer processes could also occur in S_1 state. Therefore, we conclude that both the single ESIPT process and double ESIPT process are likely to happen. So we infer the ESIPT process of this chromophore as followed: After photo-excitation, the 2HBQ-a chromophore turns to the S_1 state with the A point structure. Due to the small potential barriers, it either transfer one proton forming 2HBQ-b structure along the hydrogen bond, or it transfer both protons forming 2HBQ-c structure along both the two hydrogen bond (O_1-H_2···N_3 and O_4-H_5···N_6). The red shift in the emission spectra could be ascribed to the concomitant single ESIPT process and double ESIPT process properly.

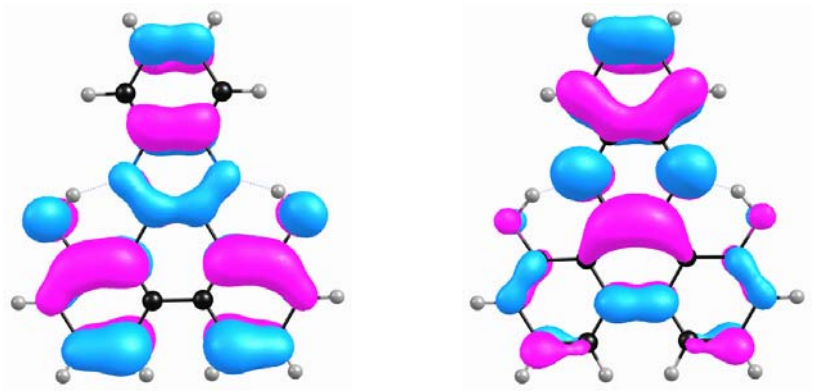

HOMO LUMO

Figure 4: The calculated frontier molecular orbitals HOMO and LUMO for 2HBQ-a at TDDFT/B3LYP/6-31+G (d) level.

4. Conclusion

In summary, we have investigated the new excited state proton transfer mechanism of 2HBQ-a chromophore based on DFT/B3LYP/6-31+G(d) calculation level in detail. Hydrogen bond strengthening of 2HBQ-a, based on primary bond lengths and IR spectra, could facilitate the proton transfer process effectively. In addition, the intramolecular charge transfer, based on the MOs, also accelerated the S_1 state ESIPT process. In fact, three kinds of stable structures of 2HBQ-a chromophore tautomerization were founded, which is different from the one proposed previously [45]. We have inferred the third structure (2HBQ-c) existing in the S_1 state theoretically, which is the deficiency in the experiment [45]. And further we proposed a new proton transfer mechanism based on the constructed PESs of the S_0 state and S_1 state. Less than 10 kcal/mol potential barriers among these excited-state minimum points demonstrated a concomitant single and double ESIPT mechanism. Based on the new ESIPT process, the phenomenon of fluorescence quenching could be explained reasonably.

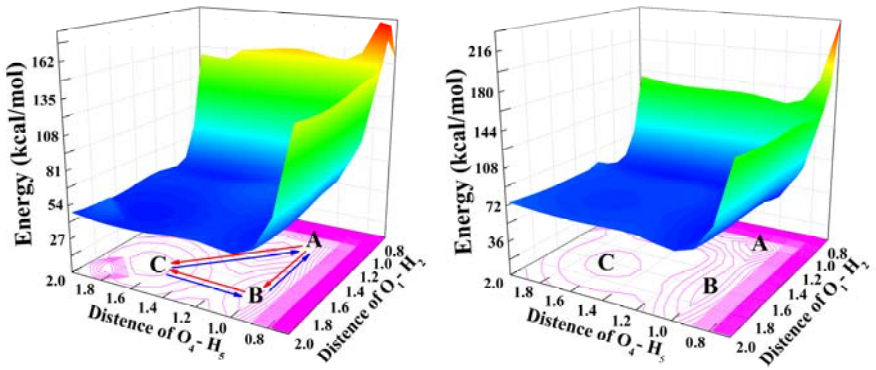

Figure 5: The constructed PESs on the S_0 and S_1 states as functions of the O_1-H_2 and O_4-H_5 lengths both from 0.69 to 1.99 Å among the 2HBQ-a structure. (a) S_1 state PES; (b) S_0 state PES. The blue and red arrows indicating the direction of the S_1 state proton transfer.

References

[1] P. L. Geissler, C. Dellago, D. Chandler, J. Hutter and M. Parrinello, Autoionization in liquid water, Science., 291 (2001), 2121-2421.

[2] M. E. Tuckerman, D. Marx and M. Parrinello, The nature and transport mechanism of hydrated hydroxide ions in aqueous solution, Nature., 417 (2002), 925-926.

[3] M. E. Tuckerman and D. Marx, Heavy-atom skeleton quantization and proton tunneling in "intermediate-barrier" hydrogen bonds, Phys. Rev. Letters., 86 (2001), 4946-4949.

[4] D. Marx, M. Tuckerman, J. Hutter and M. Parrinello, The nature of the hydrated excess proton in water, Nature., 397 (1999), 601-604.

[5] H. Chen, G. A. Voth and N. Agmon, Kinetics of proton migration in liquid water, J. Phys. Chem. B., 114 (2010), 333-339.

[6] C. Lao-Ngam, P. Asawakun, S. Wannarat and K. Sagarik, Proton transfer reactions and dynamics in protonated water clusters, Phys. Chem. Chem. Phys., 13 (2011), 21646-21647.

[7] L. Vilciauskas, M. E. Tuckerman, G. Bester, S. J. Paddison and K. D. Kreuer, The mechanism of proton conduction in phosphoric acid, Nature Chemistry., 4 (2012), 461-466.

[8] H. Beens, K. H. Grellmann, M. Gurr and A. H. Weller, Effect of solvent and tempera on proton transfer reactions of excited molecules, Discuss. Faraday Soc., 39 (1965), 183–193.

[9] A. H. Weller, Fast reactions of excited molecules, .Prog. React. Kinet., 1 (1961), 187–214.

[10] S. R. Meech, Excited state reactions in fluorescent proteins, Chem. Soc. Rev., 38 (2009), 2922-2934.

[11] P. Kukura, D. W. McCamant and R. A Mathies, Femtosecond stimulated Raman spectroscopy, Rev. Phys. Chem., 58 (2007), 461-488.

[12] T. J. Martinez, Insights for light-driven molecular devices from ab initio multiple spawning excited-state dynamics of organic and biological chromophores, Acc. Chem. Res., 39 (2006), 119-126.

[13] T. Tahara, S. Takeuchi and K. Ishii, Observation of nuclear wavepacket motion of reacting excited states in solution, J. Chin. Chem. Soc., 53 (2006), 181-189.

[14] S. Chai, G. J. Zhao, P. Song, S. Q. Yang, J. Y. Liu and K. L. Han, Reconsideration of the excited-state double proton transfer (ESDPT) in 2-aminopyridine/acid systems: role of the intermolecular hydrogen bonding in excited states, Phys. Chem. Chem. Phys., 11 (2009), 4385-4390.

[15] T. Kobayashi, T. Saito and H. Ohtani, Real-time spectroscopy of transition states in bacteriorhodopsin during retinal isomerization, Nature., 414 (2001), 531-534.

[16] S. Hayashi, E. Taikhorshid and K. Schulten, Photochemical reaction dynamics of the primary event of vision studied by means of a hybrid molecular simulation, Biophys. J., 96 (2009), 403-416.

[17] A. Sytnik and M. Kasha, Excited-state intramolecular proton-transfer as a fluorescence probe for protein binding-site static polarity, Proc. Natl. Acad. Sci. U.S.A., 91(1994), 8627-8630.

[18] Y. Kubo, S. Maeda, S. Tokita and M. Kubo, Colorimetric chiral recognition by a molecular sensor, Nature., 382 (1996), 522-524.

[19] F. B. Yu, P. Li, G. J. Zhao, T. S. Chu and K. L. Han, A near-IR reversible fluorescent probe modulated by selenium for monitoring peroxynitrite and imaging in living cells, J. Am. Chem. Soc., 133 (2011), 11030-11033.

[20] F. B. Yu, P. Li, B. S. Wang and K. L. Han, Reversible near-infrared fluorescent probe introducing tellurium to mimetic glutathione peroxidase for monitoring the redox cycles between peroxynitrite and glutathione in vivo, J. Am. Chem. Soc., 135 (2013), 7674-7690.

[21] J. S. Chen, P. W. Zhou, S. Q. Yang, A. P. Fu and T. S. Chu, Sensing mechanism for a fluoride chemosensor: invalidity of excited-state proton transfer mechanism, Phys. Chem. Chem. Phys., 15

(2013), 16183-16189.

[22] P. T. Chou, M. L. Martinez, W. C. Cooper and C. P. Chang, Photophysics of 2-(4-dialkylaminophenyl) benzothialzole-their application for near-UV laser-dyes, Appl. Spectrosc., 48 (1994), 604-606.

[23] D. G. Ma, F. S. Liang, L. X. Wang, S. T. Lee and L. S. Hung, Blue organic light-emitting devices with an oxadiazole-containing emitting layer exhibiting excited state intramolecular proton transfer, Chem. Phys. Lett., 358 (2002), 24-28.

[24] P. T. Chou, S. L. Studer and M. L. Martinez, Practical and convenient 355-nm and 337-nm sharp-cut filters for multichannel Raman- spectroscopy, Appl. Spectrosc., 45 (1991), 513-515.

[25] J. Catalan, J. C. Delvalle, F. Fabero and N. A. Garcia, The influence of molecular-conformation on the stability of ultraviolet stabilizers toward direct and dye-sensitized photoirradiation - the case of 2-(2-hydroxy-5-methyphenyl)- benzotriazole (TIN-P), Photochem. Photobiol., 61 (1995), 118-123.

[26] P. T. Chou, M. L. Martinez and S. L. Studer, The design of an effective fluorescence filter for Raman-spectroscopy, Appl. Spectrosc., 45 (1991), 918-921.

[27] J. Keck, H. E. A. Kramer, H. Port, T. Hirsch, P. Fischer and G. Rytz, Investigation on polymeric and monomeric intramolecularly hydrogen-bridged UV absorbers of the benzotriazole and triazine class, J. Phys. Chem., 100 (1996), 14468-14475.

[28] F. Vazquez, S. R. Grossman, Y. Takahshi, M. V. Rokas, N. Nakamura and W. R. Sellers, Phosphorylation of the Pten Tail acts as an inhibitory switch by preventing its recruitment into a protein complex, J. Bio. Chem., 276 (2001), 48627-48630.

[29] J. P. Xiong, R. Li, M. Essafi, T. Stehle and M. A. Arnaou, An isoleucine-based allosteric switch controls affinity and shape shifting in integrin CD11b A-domain, J. Bio. Chem., 275 (2000), 38762-38767.

[30] G. J. Zhao and K. L. Han, Novel infrared spectra for intermolecular dihydrogen bonding of the phenol-borane-trimethylamine complex in electronically excited state, J. Chem. Phys., 127 (2007), 024306-024312.

[31] G. J. Zhao and K. L. Han, Early time hydrogen-bonding dynamic of photoexcited coumarin 102 in hydrogen-donating solvents: Theoretical study, J. Phys. Chem. A., 111 (2007), 2469-2474.

[32] G. J. Zhao, J. Y. Liu, L. C. Zhou and K. L. Han, Site-selective photoinduced electron transfer from alcoholic solvents to the chromopore facilitated by hydrogen bonding: A new fluorescence quenching mechanism, J. Phys. Chem. B., 111 (2007), 8940-8945.

[33] G. J. Zhao, R. K. Chen, M. T. Sun, G. Y. Li, J. Y. Liu, Y. L. Gao, K. L. Han, X. C. Yang and L. C. Sun, Photoinduced intramolecular charge transfer and s-2 fluorescence in thiophene-pi-conjugated donor-acceptor systems: Experimental and TDDFT studieds, Chem. Eur. J., 14 (2008), 6935-6947.

[34] G. J. Zhao and K. L. Han, Hydrogen bonding in the electronic excited state, Acc. Chem. Res., 45 (2012), 404-413.

[35] G. J. Zhao and K. L. Han, Time-dependent density functional theory study on hydrogen-bonded intramolecular chage-transfer excited state of 4-dimethylamino-benzonitrile in methanol, J. Comput. Chem. 29 (2008), 2010-2017.

[36] T. Inazu, Synthesis of several gold chelates, B. Am. Chem. Soc., 39 (1966), 1065-1066.

[37] T. C. Bruice, The preparation and metal complexing of 2-(2-pyridy)-10-hydroxybenzo[h]quinoline-4-carboanillide, J. Am. Chem. Soc., 79 (1957), 702-705.

[38] S. Takeuchi and T. Tahara, Coherent nuclear wavepacket motions in ultrafast excited-state intramolecular proton transfer: Sub-30-fs resolved pump-probe absorption spectroscopy of 10-hydroxybenzo[h]quinoline in solution, J. Phys. Chem. A., 109 (2005), 10199-10207.

[39] C. Schriever, M. Barbatti, K. Stock, A. J. A. Aquino, D. Tunega, S. Lochbrunner, E. Riedle and H. Lischka, The interplay of skeletal deformations and ultrafast excited-state intramolecular proton transfer: Experimental and theoretical investigation of 10- hydroxybenzo[h]quinoline, Chem. Phys., 347 (2008), 446-461.

[40] P. T. Chou, Y. C. Chen, W. S. Yu, Y. H. Chou, C. Y. Wei and Y. M. Cheng, Excited-state intramolecular proton transfer in 10- hydroxybenzo[h]quinoline, J. Phys. Chem. A., 105 (2001), 1731-1740.

[41] P. T. Chou and C. Y. Wei, photophysics of 10- hydroxybenzo[h]quinoline in aqueous solution, J. Phys. Chem., 100 (1996), 17059-17066.

[42] E. L. Roberts, P. T. Chou, T. A. Alexander, R. A. Agbaria and I. M. Warner, Effects of organized media on the excited-state intramolecular proton-transfer of 10- hydroxybenzo[h]quinoline, J. Phys. Chem., 99 (1995), 5431-5437.

[43] M. Higashi and S. Saito, Direct simulation of excited-state intramolecular proton transfer and vibrational coherence of 10- hydroxybenzo[h]quinoline in solution, J. Phys. Chem. Lett., 2 (2011), 2366-2371.

[44] J. Lee, C. H. Kim and T. Joo, Active role of proton in excited state intramolecular proton transfer reaction, J. Phys. Chem. A., 117 (2013), 1400-1405.

[45] J. Piechowska, K. Virkki, B. Sadowski, H. Lemmetyinen, N. V. Tkachenko and D. T. Gryko, Excited state intramolecular proton transfer in pi-expanded phenazine-derived phenols, J. Phys. Chem. A., 118 (2014), 144-151.

[46] A. D. Becke, Density-functional thermochemistry .3. the role of exact exchange, J. Chem. Phys., 1993, 98, 5648-5652.

[47] C. T. Lee, W. T. Yang and R. G. Parr, Development of the colle-salvetti correlation-energy formula into a functional of the electro-density, Phys. Rev. B: Condens. Matter Mater. Phys., 37 (1988), 785-789.

[48] B. Miehlich, A. Savin, H. Stoll and H. Preuss, Result obtained with the correlation density functionals of becke and lee, yang and parr, Chem. Phys. Lett., 157 (1989), 200-206.

[49] W. Kolth, A. D. Becke and R. G. Parr, Density functional theory of electronic structure, J. Phys. Chem., 100 (1996), 12974-12980.

[50] S. H. Vosko, L. Wilk and M. Nusair, Accurate spin-dependent electron liquid correlation energies for local spin-density calculations – A critical analysis, Can J Phys., 58 (1980), 1200-1211.

[51] O. Treutler and R. Ahlrichs, Efficient molecular numerical-integration schemes, J Chem Phys., 102 (1995), 346-354.

[52] F. Furche and R. Ahlrichs, Adiabatic time-dependent density functional methods for excited state properties, J. Chem. Phys., 117 (2002), 7433-7447.

[53] M. J. Frisch, G. W. Trucks, H. B. Schlegel, G. E. Scuseria, M. A. Robb, J. R.; Scalmani, G. Cheeseman, V. Barone, B. Mennucci, G. A. Petersson, H. Nakatsuji, M. Caricato, X. Li, H. P. Hratchian, A. F. Izmaylov, J. Bloino, G. Zheng, J. L. Sonnenberg, M. Hada, M. Ehara, K. Toyota, R. Fukuda, J. Hasegawa, M. Ishida, T. Nakajima, Y. Honda, O. Kitao, H. Nakai, T. Vreven, J. A. Montgomery, Jr. J. E. Peralta, F. Ogliaro, M. Bearpark, J. J. Heyd, E. Brothers, K. N. Kudin, V. N. Staroverov, R. Kobayashi, J. Normand, K. Raghavachari, A. Rendell, J. C. Burant, S. S. Iyengar, J. Tomasi, M. Cossi, N. Rega, J. M. Millam, M. Klene, J. E. Knox, J. B. Cross, V. Bakken, C. Adamo, J. Jaramillo, R. Gomperts, R. E. Stratmann, O. Yazyev, A. J. Austin, R. Cammi, C. Pomelli, J. W. Ochterski, R. L. Martin, K. Morokuma, V. G. Zakrzewski, G. A. Voth, P. Salvador, J. Dannenberg, S. Dapprich, A. D. Daniels, O. Farkas, J. B. Foresman, J. V. Ortiz, J. Cioslowski, D. J. Fox, Gaussian 09, Revision A.02; Gaussian, Inc.: Wallingford, CT, 2009.

[54] D. Yang, Y. Yang and Y. Liu, Effect of different-type intermolecular hydrogen bonds on the geometrical and spectral properties of 6-aminocoumarin clusters in solution, Commun. Comput. Chem., 1 (2013), 205-215.

[55] J. F. Zhao, P. Song, Y. L. Cui, X. M. Liu, S. W. Sun, S. Y. Hou and F. C. Ma, Effects of hydrogen bond on 2-aminopyridine and its derivatives complexes in methanol solvent, Spectrochimica Acta Part A: Molecular and Biomolecular Spectroscopy., 131 (2014), 282-287.

[56] G. Y. Liu, Y. H. Li, H. Zhang and G. H. Cui, Time-dependent density functinal theory study on a fluorescent chemosensor based on C-H···F hydrogen-bond interaction, Commun. Comput. Chem., 1 (2013), 88-98.

[57] D. D. Wang and G. J. Zhao, Cooperatice excited-state hydrogen bond strengthening and weakening and concerted excited-state proton transfer and twisted intramolecular charge transfer of thiazolidinedione derivatives in solution, Commun. Comput. Chem., 1 (2013), 181-190.

[58] M. Z. Zhang, B. P. Ren, Y. Wang and C. X. Zhao, Excited-state intramolecular proton transfer of HDI and HBF: Excited-state hydrogen-bonding dynamics and electronic structures, Commun. Comput. Chem., 1 (2013), 216-224.

[59] Y. Liu and S. C. Lan, polarity effect of solvents on ground- and excited- state hydrogen bonds, Commun. Comput. Chem., 1 (2013), 235-243.

[60] B. Mennucci, E. Cances and J. Tomasi, Evaluation of solvent effects in isotropic and anisotropic dielectrics and in ionic solutions with a unified integral equation method: Theoretical bases, computational implementation, and numerical applications, J. Phys. Chem. B., 101 (1997), 10506-10517.

[61] E. Cances, B. Mennucci and J. Tomasi, A new intrgral equation formalism for the polarizable continuum model: Theoretical background and applications to isotropic and anisotropic dielectrics, J. Chem. Phys., 107 (1997), 3032-3041.

[62] R. Cammi and J. Tomasi, Remarks on the use of the apparent surface-charges (ASC) methods in salvation problems-iterative versus matrix-inversion procedures and the renormalization of the apparent charges, J. Comput. Chem., 16 (1995), 1449-1458.

[63] S. Miertus, E. Scrocco and J. Tomasi, Electrostatic interaction of a solute with a continuum-a direct utilization of ab initio molecular potentials for the prevision of solvent effects, J. Chem. Phys., 55 (1981), 117-129.

[64] L. Serrano-Andres and M. Merchan, Are the five natural DNA/RNA base monomers a good choice from natural selection? A photochemical perspective, J. Photochem. Photobiol. C. Photochem. Rev., 10 (2009), 21-32.

[65] Y. Saga, Y. Shibata and H. Tamiaki, Spectral properties of single light-harvesting complexes in bacterial photosynthesis, J. Photochem. Photobiol. C. Photochem. Rev., 11 (2010), 15-24.

[66] A. L. Sobolewski and W. Domcke, Ab initio potential-energy functions for excited state intramolecular proton transfer: a comparative study of o-hydroxybenzaldehyde, salicylic acid and 7-hydroxy-1-indanone, Phys. Chem. Chem. Phys., 1 (1999), 3065-3072.